NOTE

Magnetic Resonance in Medicine 00:00–00 (2013)

3D Late Gadolinium Enhancement in a Single Prolonged Breath-hold using Supplemental Oxygenation and Hyperventilation

Sébastien Roujol,[1] Tamer A. Basha,[1] Mehmet Akçakaya,[1] Murilo Foppa,[1] Raymond H. Chan,[1] Kraig V. Kissinger,[1] Beth Goddu,[1] Sophie Berg,[1] Warren J. Manning,[1,2] and Reza Nezafat[1]*

Purpose: To evaluate the feasibility of three-dimensional (3D) single breath-hold late gadolinium enhancement (LGE) of the left ventricle (LV) using supplemental oxygen and hyperventilation and compressed-sensing acceleration.

Methods: Breath-hold metrics [breath-hold duration, diaphragmatic/LV position drift, and maximum variation of R wave to R wave (RR) interval] without and with supplemental oxygen and hyperventilation were assessed in healthy adult subjects using a real-time single shot acquisition. Ten healthy subjects and 13 patients then underwent assessment of the proposed 3D breath-hold LGE acquisition (field of view = 320 × 320 × 100 mm^3, resolution = 1.6 × 1.6 × 5.0 mm^3, acceleration rate of 4) and a free-breathing acquisition with right hemidiaphragm navigator (NAV) respiratory gating. Semiquantitative grading of overall image quality, motion artifact, myocardial nulling, and diagnostic value was performed by consensus of two blinded observers.

Results: Supplemental oxygenation and hyperventilation increased the breath-hold duration (35 ± 11 s to 58 ± 21 s; $P < 0.0125$) without significant impact on diaphragmatic/LV position drift or maximum variation of RR interval (both $P > 0.01$). LGE images were of similar quality when compared with free-breathing acquisitions, but with reduced total scan time (85 ± 22 s to 35 ± 6 s; $P < 0.001$).

Conclusions: Supplemental oxygenation and hyperventilation allow for prolonged breath-holding and enable single breath-hold 3D accelerated LGE with similar image quality as free breathing with NAV. **Magn Reson Med 000:000–000, 2013.**

Key words: late gadolinium enhancement; myocardial viability; 3D acquisition; acceleration techniques; breath-hold; left ventricle; hyperventilation; compressed sensing

INTRODUCTION

Late gadolinium enhancement (LGE) MRI allows for non-invasive assessment of fibrosis and scar (1,2). Two-dimensional (2D) multislice LGE is commonly used for the clinical assessment of left ventricular (LV) scar/fibrosis (2). A series of 10–14 short-axis slices is necessary to cover the entire LV and is acquired in 5–7 consecutive breath-holds (n = 2 slices per breath-hold). However, 2D multislice acquisitions are limited by a large (8- to 10-mm) slice thickness that leads to partial volume effects and slice registration errors due to variability of breath-holds. Three-dimensional (3D) LGE sequences provide a higher signal-to-noise ratio and can thus be used to increase LGE spatial resolution, especially in the through-plane direction, leading to improved scar quantification (3,4) when compared with 2D acquisitions.

Due to their long acquisitions, 3D LGE acquisitions are most commonly performed using free breathing (5–9) with right hemidiaphragm (RHD) respiratory navigators (NAVs) (5–8). However, free-breathing NAV-gated 3D LGE results in prolonged scan times due to NAV inefficiency. Drift of the respiratory pattern can also be observed, leading to poor gating efficiency and potentially incomplete scans. Furthermore, application of the NAV restore pulse in LGE causes additional inflow artifacts (10). Finally, due to contrast washout kinetics over the whole acquisition, the optimal inversion time to null healthy myocardial signal may shift over the duration of the prolonged acquisition and result in additional image artifacts. 3D phase-sensitive inversion recovery sequences (11) eliminates the sensitivity to an imperfect inversion time (11,12). However, this approach increases the scan time by a factor of 2, which is not desired in 3D imaging. As an alternative, self-gated acquisitions have been proposed where the acquired image data are directly used for respiratory motion estimation and gating. Although self-gating techniques have been applied successfully in several applications such as CINE (13) and coronary MR angiography (14,15), it has not yet been applied to 3D LGE imaging and remains challenging due to the temporal variation of the LGE signal.

3D breath-hold acquisitions covering the entire LV have been proposed for LGE but are associated with relatively low spatial resolution due to the limitation of breath-hold duration (3,16–18). Segmented 3D breath-hold acquisitions where the LV dataset is acquired in

Additional Supporting Information may be found in the online version of this article.

[1]Department of Medicine (Cardiovascular Division), Beth Israel Deaconess Medical Center and Harvard Medical School, Boston, Massachusetts, USA.
[2]Department of Radiology, Beth Israel Deaconess Medical Center and Harvard Medical School, Boston, Massachusetts, USA.

Grant sponsor: National Institutes of Health; Grant number: R01EB008743-01A2.

*Correspondence to: Reza Nezafat, Ph.D., Beth Israel Deaconess Medical Center, 330 Brookline Ave, Boston, MA, 02215.
E-mail: rnezafat@bidmc.harvard.edu

Received 26 March 2013; revised 28 August 2013; accepted 4 September 2013
DOI 10.1002/mrm.24969
Published online 00 Month 2013 in Wiley Online Library (wileyonlinelibrary.com).

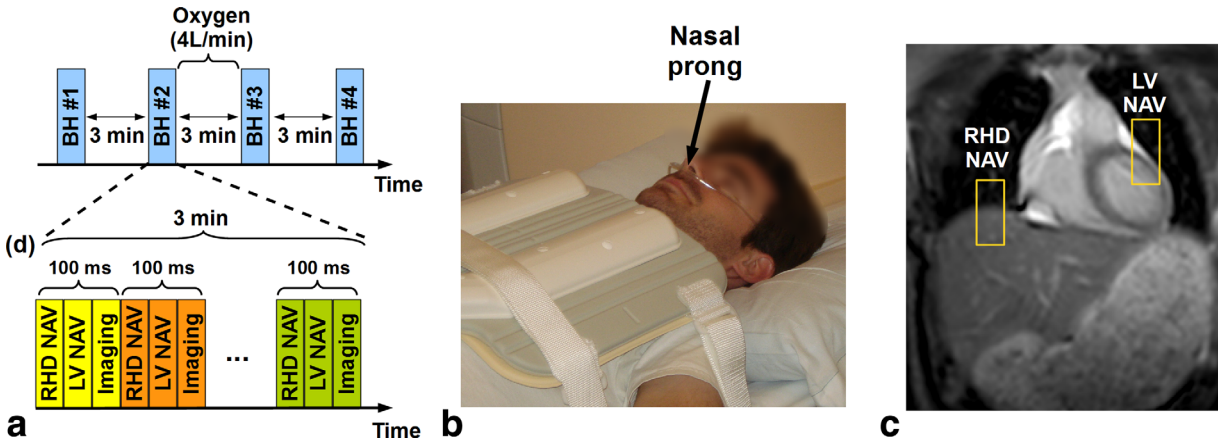

FIG. 1. Imaging protocol for breath-hold (BH) assessment. **a:** Study protocol designed for breath-hold assessment without (BH#1, BH#2, and BH#4) and with (BH#3) supplemental oxygen and hyperventilation. **b:** Oxygen (4 L/min) was administrated using nasal prolong. **c, d:** Sequence diagram used for breath-hold monitoring. A real-time steady-state free precession sequence was used to acquire a complete image every 100 ms using an RHD NAV, a NAV located at the left ventricle LV (LV NAV), and a 2D coronal imaging slice (Imaging).

three separate breath-holds has been proposed, but may lead to misalignment of the 3D volumes due to breath-hold variations (19). As a result, single breath-holds using a highly accelerated 3D acquisition would be desirable. Parallel imaging techniques such as SENSE (20) or GRAPPA (21) are widely available and have been used in 3D and 2D LGE with acceleration rates of up to 2 (22–25). Compressed sensing (CS) (26,27) is an alternative acceleration technique that enables higher acceleration rates. The use of CS to accelerate LGE acquisitions by a factor of 4 has been presented recently (28). Prolonged breath-hold duration may also enable longer acquisition time and increased spatial resolution. Supplemental oxygen combined with hyperventilation has been demonstrated to provide substantially longer breath-hold durations (29–32).

In this study, we sought to investigate the feasibility of a highly accelerated LGE acquisition in combination with a prolonged breath-hold facilitated by supplemental oxygenation and hyperventilation. The contribution of this study is twofold. Initially, we assessed the impact of supplemental oxygenation and hyperventilation on breath-hold duration, diaphragmatic/LV position drift, and maximum variation of R wave to R wave (RR) interval during breath-hold in healthy subjects. Subsequently, the feasibility of a single breath-hold accelerated 3D LGE acquisition was demonstrated using supplemental oxygenation, hyperventilation, and CS-based acceleration technique.

METHODS

All imaging was performed on a 1.5T Philips Achieva (Philips Healthcare, Best, The Netherlands) scanner using a 32-channel cardiac phased array receiver coil. Written informed consent was obtained from all participants, and the imaging protocol was approved by our institutional review board.

Breath-hold metrics (breath-hold duration, diaphragmatic position drift, LV position drift, and maximum variation of RR interval) were analyzed using a combination of real-time imaging and monitoring of motion using respiratory NAVs,. Subsequently, the feasibility of single breath-hold 3D LGE imaging with supplemental oxygenation and hyperventilation was studied.

Breath-hold Characterization without and with Supplemental Oxygenation and Hyperventilation

Ten healthy adult subjects (healthy group #1; age, 29 ± 15 yr; male, $n = 3$; female, $n = 7$) without any history of cardiovascular disease underwent MRI without and with supplemental oxygenation and hyperventilation. Figure 1 shows the imaging protocol used to evaluate breath-hold characteristics. In each subject, four different breath-hold scans were performed at end expiration (Fig. 1a). End-inspiration breath-holds were not assessed because they are associated with more complex motion drift/variation (33), which is undesirable for 3D LGE imaging. For the purpose of training, all subjects were asked to perform an initial breath-hold (BH#1) without supplemental oxygenation or hyperventilation. Subsequently, two breath-hold scans were performed without (BH#2) and with (BH#3) supplemental oxygenation and hyperventilation. Supplemental oxygen (4 L/min, nasal prongs) was administered for 3 minutes (Fig. 1b). Hyperventilation was performed immediately before the breath-hold by instructing the subject to take three rapid maximum capacity respirations. A fourth breath-hold scan was then performed without supplemental oxygenation or hyperventilation (BH#4). The interval between each breath-hold was 3 minutes to allow for subject recovery. In each breath-hold, subjects were asked to sustain their end-expiratory breath-hold as long as possible. To demonstrate whether the increased breath-hold duration is associated with supplemental oxygen or a placebo effect, we repeated a similar study in a separate group of 10 healthy subjects (healthy group #2; age, 32 ± 17 yr; male, $n = 1$; female, $n = 9$). In this study, subjects were not instructed for hyperventilation and were told they would receive supplemental oxygen; however, room air (4 L/min during 3 minutes) was administered.

A 2D dynamic real time sequence was acquired during each breath-hold for both subject groups. Two pencil-beam NAVs positioned on the dome of the RHD and the LV (Figure 1c) were acquired for each dynamic with a temporal resolution of 17 ms each. NAVs were positioned in superior inferior direction and employed a 2D spiral pulse using the following parameters: spatial resolution = 1 mm; flip angle = 25°; echo time (TE) = 1.2 ms; bandwidth = 54 kHz. These NAV acquisitions were followed by a 2D dynamic real-time steady-state free precession (SSFP) acquisition using the following parameters: pulse repetition time (TR)/TE/α = 2 ms/1 ms/50°; field of view = 320 × 320 mm^2; spatial resolution = 3.9 × 3.9 mm^2; slice thickness = 10 mm; SENSE factor = 2.35 (Fig. 1d). The total scan time for the two NAVs and real-time SSFP was 100 ms. This acquisition scheme was repeated continuously for 3 min (1800 dynamics) to monitor the patient breathing pattern during and immediately after breath-hold. The 2D images were not used for breath-hold characteristic assessment, which was only based on the analysis of the two respiratory NAVs and the recorded electrocardiographic (ECG) signal.

NAVs and ECG signals of each acquisition were exported from the scanner and analyzed in MATLAB (Mathworks, Natick, Massachusetts, USA). Breath-hold duration was measured by visual identification of the stable period of the RHD NAV signal. The diaphragmatic position drift was measured as the difference between the maximum and minimum RHD position over the breath-hold period. Because the LV NAV contains cardiac motion preventing an accurate detection of the respiratory induced drift, a third-order polynomial fit of the signal was first performed to remove the influence of the cardiac motion. The LV position drift was then measured as the difference between the maximum and minimum of the LV NAV fitted signal over the breath-hold period. The ECG R-wave was used to calculate the maximum variation of RR interval of each subject through each scan.

3D LGE Imaging

The 10 healthy subjects from healthy group #1 and 13 patients (age, 53 ± 12 yr; male, n = 9; female, n = 4) referred to our center for evaluation of cardiovascular disease were recruited for this imaging study. Each subject was imaged for evaluation of scar using 1) free-breathing LGE using RHD NAV and 2) breath-hold LGE with supplemental oxygen and hyperventilation. Two scans were acquired in a random order to account for differences in contrast washout. LGE acquisitions were performed 16 ± 4 min (in healthy subjects) and 21 ± 8 min (in patients) after administration of 0.1 or 0.2 mmol/kg of gadobenate dimeglumine (MultiHance; Bracco Diagnostic Inc., Princeton, New Jersey, USA). To comply with our institutional review board's requirements, subjects with an estimated glomerular filtration rate of 45–60 mL/min/1.73 m^2 only received 0.1 mmol/kg of gadobenate dimeglumine. All healthy subjects and five of 13 patients received an injection of 0.2 mmol/kg gadobenate dimeglumine. Eight patients received a single dose of 0.1 mmol/kg gadobenate dimeglumine. Before each 3D LGE acquisition, a Look-Locker sequence (34) was performed to obtain the optimal inversion time to provide the best nulling of the LV myocardium signal. Two 3D ECG-triggered inversion recovery prepared spoiled gradient echo sequences were used for LGE imaging with the following parameters: TR/TE/α = 5.2 ms/2.6 ms/25°, field of view = 320 × 320 × 100 mm^3, acquisition matrix = 200 × 200 × 25, resulting in a spatial resolution of 1.6 × 1.6 × 5.0 mm^3, and acquisition in every heartbeat (1 RR). All images were acquired during diastolic rest period with average duration of 126 ms (25 k-space lines) for healthy subjects and 146 ms (29 k-space lines) for patients. Both sequences used a four-fold CS acceleration rate. The free-breathing 3D LGE sequence employed a RHD NAV for gating and tracking the respiratory motion [gating window = 7 mm, tracking factor = 0.6 (35)]. The breath-hold LGE sequence was performed with supplemental oxygenation (4 L/min for 3 minutes by nasal prong) and hyperventilation (three rapid maximum capacity breathes immediately before the end-expiratory breath-hold.

To accelerate imaging, a randomly undersampled pattern was developed for 3D LGE. The undersampling pattern was designed to fully acquire the k-space center lines and to randomly discard lines from the outer k-space so as to reach the desired acceleration factor. The number of k-space center lines fully acquired was set to 21 × 9 lines (k_y-k_z). An identical randomly undersampled k-space profile was used for all the studies to minimize the effect of k-space weighting due to signal recovery after the inversion pulse in LGE. The raw k-space data were extracted, and all image reconstructions were performed off-line using an improved CS reconstruction technique (36).

In a prior contrast-enhanced coronary (36) and LGE study (28), a radial k-space profile reordering (Supporting Fig. 1, left) was used to minimize the gradient jumps induced by the random pattern of the outer k-space (36). The acquisition is started with the blue segments and finished with the outer red segments. In this study, we propose an alternative profile reordering technique in which the center of k-space is acquired in a linear fashion immediately after the initiation of data acquisition (Supporting Fig. 1, right). The remaining outer k-space segments are then acquired in a radial fashion. This profile ordering provides improved robustness against motion, respiratory motion drift, and incomplete breath-holds and is referred to as "inner linear-outer radial profile reordering."

Data Analysis

The statistical significance between breath-holds was evaluated for each metric using one-way analysis of variance (ANOVA) with a significance threshold of $P < 0.05$. Additional paired *t* tests with Bonferroni correction were performed for all pairs of breath-holds when the ANOVA test was found significant. Statistical significance was considered at $P < 0.05/6 \approx 0.008$.

Reconstructed images obtained from the healthy adult subjects and the patients were exported in DICOM

Table 1
Breath-hold Duration, RHD Position Drift, LV Position Drift and Maximal Variation of RR Interval Variation Measured from the Breath-holds Performed in a Sequential Order without (BH#1, BH#2, BH#4) and with (BH#3) Supplemental O_2 (4 L/min Nasal Prong) and Hyperventilation in 10 Healthy Adult Subjects (Healthy Group #1)

	Breath-Hold Duration (s)	RHD Position Drift (mm)	LV Position Drift (mm)	Maximum Variation of RR Interval (bpm)
BH#1	35 ± 11 (18–53)	4.6 ± 3.3 (1–10)	2.7 ± 2.1 (0–8)	12 ± 6 (5–25)
BH#2	40 ± 14 (18–65)	5.9 ± 4.0 (2–15)	3.8 ± 2.3 (1–9)	14 ± 8 (5–30)
BH#3	58 ± 21 (27–96)	7.0 ± 4.6 (1–18)	4.9 ± 3.9 (2–12)	13 ± 5 (8–25)
BH#4	41 ± 16 (14–60)	6.9 ± 4.2 (3–16)	3.4 ± 2.7 (1–9)	14 ± 5 (8–20)
$P_{BH\ \#1\ vs.\ \#2}$	0.015	NS	NS	NS
$P_{BH\ \#2\ vs.\ \#3}$	0.005	NS	NS	NS
$P_{BH\ \#3\ vs.\ \#4}$	0.007	NS	NS	NS
$P_{BH\ \#2\ vs.\ \#4}$	NS	NS	NS	NS

Minimum and maximum values are given in parentheses. The duration of the second breath-hold (BH#2; no supplemental O_2 or hyperventilation) was longer than that of the first breath-hold, confirming the benefit of a training breath-hold with no further benefit of training (BH#4). Still longer breath-holds were achieved with supplemental O_2 and hyperventilation (BH#3). NS, not significant.

format and loaded into the Synedra View Personal (Synedra Information Technologies GmbH, Aachen, Germany) for image visualization and analysis. A subjective qualitative assessment of image quality was performed by consensus of two experienced cardiologists blinded to the acquisition scheme and all patient data. Each 3D dataset was scored for diagnostic value (yes/no) and image quality based on a 4-point scale: 1 = poor/uninterpretable (severe motion/blurring artifact or poor nulling of the myocardium); 2 = fair (moderate motion/blurring artifact or imperfect nulling of the myocardium); 3 = good (mild motion/blurring artifact and good nulling of the myocardium); 4 = excellent (sharply defined myocardium without motion/blurring artifact and excellent myocardial nulling). Motion artifact and myocardial nulling were also individually scored based on the same 4-point scale corresponding to each of these criteria. A Wilcoxon signed rank test was used to test the null hypothesis that the difference of image quality scores between both acquisitions was zero. Diagnostic values were compared between both sequences by means of McNemar's test. Statistical significance was considered for $P < 0.05$.

RESULTS

Breath-hold Characterization

Examples of RHD NAV data, LV NAV data, and RR interval variation are shown in Supporting Figure 2 during breath-holds without (Supporting Fig. 2a, 2c, and 2e) and with (Supporting Fig. 2b, 2d, and 2f) supplemental oxygenation and hyperventilation. Table 1 summarizes the breath-hold characteristics for all subjects of healthy group #1. One-way ANOVA indicated statistical difference in term of breath-hold duration among the breath-holds ($P = 0.02$). Additional paired t tests revealed statistical differences between BH#1 versus BH#3 ($P = 0.001$), BH#2 versus BH#3 ($P = 0.005$), and BH#4 versus BH#3 ($P = 0.007$) demonstrating that supplemental oxygenation and hyperventilation significantly prolong breath-hold duration by ~20 s. There was a trend for the second to be longer than the first breath-hold (~5 s, $P = 0.015$) suggesting the use of a training breath-hold. One breath-hold has been found sufficient for the training phase since no further increase was observed between the second and the fourth breath-hold ($P = 0.79$). Finally, there were no statistically significant differences between breath-holds for all remaining metrics as determined by the one-way ANOVA ($P > 0.05$ for all metrics). Finally, in the healthy group #2, breath-hold duration was 34 ± 12 s, 35 ± 13 s, 38 ± 13 s, and 36 ± 14 s for BH#1, BH#2, BH#3, and BH#4, respectively. No significant difference was observed between breath-holds in terms of breath-hold duration as indicated by one-way ANOVA ($P = 0.94$).

3D LGE Imaging: Free-Breathing versus Breath-hold Acquisitions

Figure 2 shows examples of 3D LGE images, acquired in three healthy subjects and three patients with both breath-hold and free-breathing acquisitions. Image quality obtained for both acquisitions appears similar in term of sharpness and motion/blurring artifact. Figure 3 shows two slices from the 3D LGE dataset acquired in a 44-year-old patient with a prior myocardial infarction using both free-breathing and breath-hold acquisitions. Both acquisitions were performed 45 minutes after injection of only 0.1 mmol/kg of contrast agent which resulted in reduced overall contrast when compared with other patient data in Figure 2. The free-breathing acquisition was completed in 2 min, 26 s (25% gating efficiency). Severe motion artifacts are visible in all slices limiting accurate delineation of the scar area. The proposed 3D breath-hold LGE provided improved image quality where the scar area could be defined in all slices.

Table 2 summarizes the data from the healthy subjects, the patients, and the combined group. LGE signal enhancement was observed in only two patients. 3D LGE images were identified as diagnostic in all healthy subjects using both 3D LGE sequences. Three of 13 (23%) patients had nondiagnostic images using both acquisitions. Note that myocardial nulling was scored either 1 or 2 for both techniques in these three patients. Two additional patients had nondiagnostic images using the free-breathing acquisition and diagnostic images using the proposed 3D breath-hold LGE sequence. No significant difference was found between the two sequences in

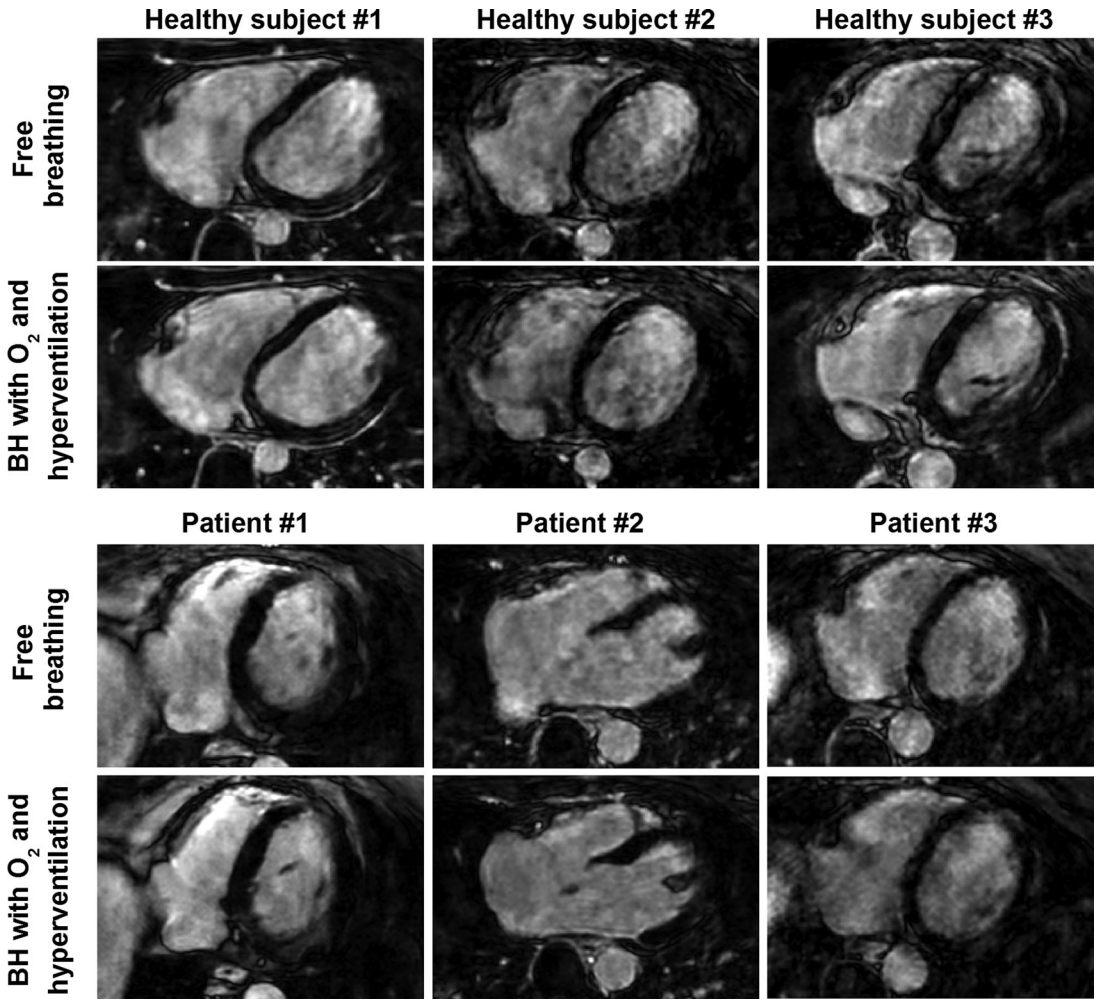

FIG. 2. 3D axial LGE images (undersampling rate = 4) obtained in three healthy subjects and three patients using the breath-hold (BH) acquisition with supplemental oxygenation (O_2) and hyperventilation and the free-breathing acquisition. Similar image quality was obtained using both sequences.

terms of diagnostic value, motion artifact, and myocardial nulling. Overall image quality in all subjects (healthy and patients) was similar for breath-hold LGE and free-breathing LGE (P value not significant). Breath-hold LGE significantly reduced the overall scan time from 85 ± 22 s (free-breathing LGE) to 35 ± 6 s ($P < 0.001$).

DISCUSSION

In this study, we demonstrated the feasibility of a single breath-hold 3D LGE acquisition using a highly accelerated acquisition combined with supplemental oxygen and hyperventilation. The latter led to prolonged breath-holding performance in both healthy adults and patients with cardiovascular disease. For both healthy subjects and patients, the single breath-hold 3D LGE images were of similar quality when compared with a more conventional free-breathing 3D respiratory NAV acquisition.

We observed a >50% increase in breath-hold duration when the breath-hold is performed with hyperventilation and supplemental oxygen. A finding in good agreement with prior data from Danias et al. (29) who noted an increase from 35 to 55 s in similar conditions. In the current study, we also observed that breath-hold training could provide an increase in breath-hold duration; however, these results would need to be confirmed in a larger subject group. We also showed that increase in breath-hold duration is attributed to supplemental oxygenation and hyperventilation of the subject and not to a placebo effect. These data suggest that supplemental oxygen and hyperventilation should be considered routine for optimum prolonged breath-hold performance and that a training breath-hold is beneficial.

Diaphragmatic position drift data were also in good agreement with published data of 6.6 ± 3.5 mm (29). Despite our instructions for an end-expiratory breath-hold, NAV data demonstrated that our subject with the largest (18 mm) RHD drift held their breath at end-inspiration.

Inversion recovery LGE sequences are sensitive to RR interval variation. We found no significant difference in maximum variation of RR interval with supplemental oxygen and hyperventilation. These data will need to be confirmed in a larger study.

Compared with previous 3D breath-hold LGE approaches where the resolution in the third dimension

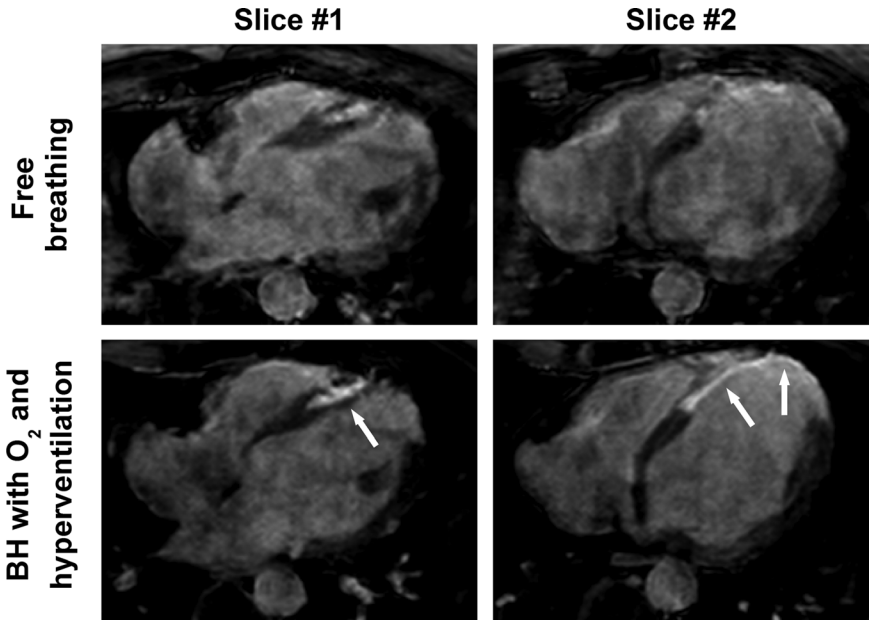

FIG. 3. 3D axial LGE images (undersampling rate = 4) obtained in a 44-year-old gentleman with a history of myocardial infarction using free-breathing NAV acquisition and breath-hold acquisition with supplemental oxygen and hyperventilation. A 25% NAV gating efficiency resulted in total scan time of 2 min, 26 s with images showing motion artifacts and incomplete myocardial nulling. The proposed 3D breath-hold (BH) LGE acquisition with supplemental oxygenation and hyperventilation provided better image quality with substantially reduced motion artifacts and myocardial nulling, allowing for better LGE assessment.

was >8 mm (3,17,18) using a relatively long acquisition window (180 ms to 326 ms) which are sensitive to motion artifacts, the proposed approach allows for increasing the resolution in the third dimension by a factor of ~2 while maintaining a shorter acquisition window of ~120 ms. Our MRI parameters also include a slightly longer TR (5.2 ms) when compared with prior 3D breath-hold LGE studies [3.8–4.2 ms (3,17,18)] which is expected to result in better signal-to-noise ratio. Signal-to-noise ratio was not examined in our study due to CS reconstruction.

The employed inner linear-outer radial profile ordering technique allows for a virtual acquisition of the k-space center lines within a narrow gating window. Although this profile reordering technique is expected to improve the robustness of the acquisition against RR interval variation, this was not evaluated in the study.

The scan time of the single breath-hold 3D LGE is approximately ~35 s with 1.6 × 1.6 × 5 mm^3 spatial resolution and acquisition window of 120 ms. Although all healthy subjects and patients could sustain such long breath-hold, the proposed technique may not be applicable in all patients. For example, patients with chronic obstructive pulmonary disease or congestive heart failure may show reduced breath-holding abilities (37). Further acceleration is required to enable breath-hold 3D LGE in these patients. For patients who are unable to hold their breath, the free-breathing 3D LGE with NAV gating can still be used.

Quantitative or semiquantitative assessment of LGE scar, including transmurality, scar volume, and the size of the peri-infarct zone have been widely used as metrics, with potential prognostic value (38). Higher spatial resolution LGE (28) could potentially improve our ability to better quantify these metrics; however, higher-resolution imaging is long and may not be needed if the patient does not have any scar. Thus, the proposed approach may have a role as an initial survey scan to

Table 2
Diagnostic Value, Image Quality, and Acquisition Time Using Free-Breathing and 3D Breath-hold LGE

	Diagnostic (yes)	Image Quality			Acquisition Time (s)
		Overall Quality (1–4)	Motion Artifact (1–4)	Myocardial Nulling (1–4)	
Healthy					
Free-breathing LGE	10/10	3.7 ± 0.5	3.7 ± 0.5	4.0 ± 0.0	81 ± 12
Breath-hold LGE	10/10	3.8 ± 0.4	3.8 ± 0.4	4.0 ± 0.0	37 ± 6
P value	NS	NS	NS	NS	<0.001
Patient					
Free-breathing LGE	8/13	2.7 ± 0.8	3.1 ± 0.8	3.1 ± 1.3	88 ± 28
Breath-hold LGE	10/13	3.1 ± 0.7	3.4 ± 0.6	3.2 ± 1.2	34 ± 6
P value	NS	NS	NS	NS	<0.001
Overall					
Free-breathing LGE	18/23	3.1 ± 0.9	3.3 ± 0.8	3.5 ± 1.1	85 ± 22
Breath-hold LGE	20/23	3.4 ± 0.7	3.6 ± 0.6	3.5 ± 1.0	35 ± 6
P value	NS	NS	NS	NS	<0.001

Similar image quality is achieved using both sequences, whereas 3D BH LGE provides a significant reduction of acquisition time. NS, not significant.

determine the presence/absence of scar before initiating a longer dedicated 3D high-resolution scan. This will save 5–12 min of scan time in our current imaging protocol for scar assessment.

The physiology of breath-holding involves a complex mechanism driven by O_2 and CO_2 partial pressures in blood, which are detected by chemoreceptors in arteries and the central nervous system (39–41). During breath-hold, the arterial pressure of oxygen falls while the CO_2 pressure increases. One hypothesis explaining breath-hold breakpoint is the detection of too low oxygen arterial partial pressure or too high CO_2 arterial pressure which would generate an involuntary breath. This hypothesis thus suggests the existence of a minimum O_2 arterial pressure threshold and a maximum CO_2 arterial pressure threshold. Supplemental oxygen may increase its partial pressure in the blood. Moreover, the hyperventilation induces a reduction of the CO_2 level in the blood (hypocapnia), which has an important role, as hypoxemia is thought to be less dyspnea-inducing than hypercapnia (39,40).

There are several limitations in this study. Variations in sex, age, contrast agent dose, and imaging time among healthy subjects and patients could have limited the assessment of differences in breath-hold metrics and LGE sequences. Our patient population was small and the impact of supplemental oxygen and hyperventilation needs to be further examined within the context of a much broader range of patients with cardiovascular disease. The number of subjects with LGE fibrosis/scar was small and also needs to be confirmed in a larger series, as well as reproducibility of the prolonged single breath-hold compared with RHD NAV gating. No quantitative LGE analysis was performed. Finally, we did not compare the breath-hold 3D LGE approach to conventional breath-hold 2D acquisitions.

CONCLUSION

Supplemental oxygenation and hyperventilation increase breath-hold duration by a factor of >1.5 without significant changes of diaphragm/LV position drift and maximum variation of RR interval. The proposed single breath-hold 3D accelerated LGE imaging using supplemental oxygenation and hyperventilation provides similar image quality as free-breathing 3D accelerated LGE imaging with respiratory gating/tracking.

REFERENCES

1. Kim RJ, Wu E, Rafael A, Chen EL, Parker MA, Simonetti O, Klocke FJ, Bonow RO, Judd RM. The use of contrast-enhanced magnetic resonance imaging to identify reversible myocardial dysfunction. N Engl J Med 2000;343:1445–1453.
2. Simonetti OP, Kim RJ, Fieno DS, Hillenbrand HB, Wu E, Bundy JM, Finn JP, Judd RM. An improved MR imaging technique for the visualization of myocardial infarction. Radiology 2001;218:215–223.
3. Goetti R, Kozerke S, Donati OF, Surder D, Stolzmann P, Kaufmann PA, Luscher TF, Corti R, Manka R. Acute, subacute, and chronic myocardial infarction: quantitative comparison of 2D and 3D late gadolinium enhancement MR imaging. Radiology 2011;259:704–711.
4. Peters DC, Appelbaum EA, Nezafat R, Dokhan B, Han Y, Kissinger KV, Goddu B, Manning WJ. Left ventricular infarct size, peri-infarct zone, and papillary scar measurements: a comparison of high-resolution 3D and conventional 2D late gadolinium enhancement cardiac MR. J Magn Reson Imaging 2009;30:794–800.
5. Nguyen TD, Spincemaille P, Weinsaft JW, Ho BY, Cham MD, Prince MR, Wang Y. A fast navigator-gated 3D sequence for delayed enhancement MRI of the myocardium: comparison with breathhold 2D imaging. J Magn Reson Imaging 2008;27:802–808.
6. Saranathan M, Rochitte CE, Foo TK. Fast, three-dimensional free-breathing MR imaging of myocardial infarction: a feasibility study. Magn Reson Med 2004;51:1055–1060.
7. Goldfarb JW, Shinnar M. Free-breathing delayed hyperenhanced imaging of the myocardium: a clinical application of real-time navigator echo imaging. J Magn Reson Imaging 2006;24:66–71.
8. Spuentrup E, Buecker A, Karassimos E, Gunther RW, Stuber M. Navigator-gated and real-time motion corrected free-breathing MR Imaging of myocardial late enhancement. Rofo 2002;174:562–567.
9. Peters DC, Shaw JL, Knowles BR, Moghari MH, Manning WJ. Respiratory bellows-gated late gadolinium enhancement of the left atrium. J Magn Reson Imaging 2012. doi: 10.1002/jmri.23954.
10. Moghari MH, Peters DC, Smink J, Goepfert L, Kissinger KV, Goddu B, Hauser TH, Josephson ME, Manning WJ, Nezafat R. Pulmonary vein inflow artifact reduction for free-breathing left atrium late gadolinium enhancement. Magn Reson Med 2011;66:180–186.
11. Kellman P, Arai AE, McVeigh ER, Aletras AH. Phase-sensitive inversion recovery for detecting myocardial infarction using gadolinium-delayed hyperenhancement. Magn Reson Med 2002;47:372–383.
12. Huber AM, Schoenberg SO, Hayes C, Spannagl B, Engelmann MG, Franz WM, Reiser MF. Phase-sensitive inversion-recovery MR imaging in the detection of myocardial infarction. Radiology 2005;237:854–860.
13. Larson AC, White RD, Laub G, McVeigh ER, Li D, Simonetti OP. Self-gated cardiac cine MRI. Magn Reson Med 2004;51:93–102.
14. Lai P, Larson AC, Park J, Carr JC, Li D. Respiratory self-gated four-dimensional coronary MR angiography: a feasibility study. Magn Reson Med 2008;59:1378–1385.
15. Stehning C, Bornert P, Nehrke K, Eggers H, Stuber M. Free-breathing whole-heart coronary MRA with 3D radial SSFP and self-navigated image reconstruction. Magn Reson Med 2005;54:476–480.
16. Dewey M, Laule M, Taupitz M, Kaufels N, Hamm B, Kivelitz D. Myocardial viability: assessment with three-dimensional MR imaging in pigs and patients. Radiology 2006;239:703–709.
17. Foo TK, Stanley DW, Castillo E, Rochitte CE, Wang Y, Lima JA, Bluemke DA, Wu KC. Myocardial viability: breath-hold 3D MR imaging of delayed hyperenhancement with variable sampling in time. Radiology 2004;230:845–851.
18. Kuhl HP, Papavasiliu TS, Beek AM, Hofman MB, Heusen NS, van Rossum AC. Myocardial viability: rapid assessment with delayed contrast-enhanced MR imaging with three-dimensional inversion-recovery prepared pulse sequence. Radiology 2004;230:576–582.
19. Bauner KU, Muehling O, Theisen D, Hayes C, Wintersperger BJ, Reiser MF, Huber AM. Assessment of myocardial viability with 3D MRI at 3 T. AJR Am J Roentgenol 2009;192:1645–1650.
20. Pruessmann KP, Weiger M, Scheidegger MB, Boesiger P. SENSE: sensitivity encoding for fast MRI. Magn Reson Med 1999;42:952–962.
21. Griswold MA, Jakob PM, Heidemann RM, Nittka M, Jellus V, Wang J, Kiefer B, Haase A. Generalized autocalibrating partially parallel acquisitions (GRAPPA). Magn Reson Med 2002;47:1202–1210.
22. van den Bosch HC, Westenberg JJ, Post JC, Yo G, Verwoerd J, Kroft LJ, de Roos A. Free-breathing MRI for the assessment of myocardial infarction: clinical validation. AJR Am J Roentgenol 2009;192:W277–W281.
23. Kellman P, Larson AC, Hsu LY, Chung YC, Simonetti OP, McVeigh ER, Arai AE. Motion-corrected free-breathing delayed enhancement imaging of myocardial infarction. Magn Reson Med 2005;53:194–200.
24. McGann CJ, Kholmovski EG, Oakes RS, et al. New magnetic resonance imaging-based method for defining the extent of left atrial wall injury after the ablation of atrial fibrillation. J Am Coll Cardiol 2008;52:1263–1271.
25. Oakes RS, Badger TJ, Kholmovski EG, et al. Detection and quantification of left atrial structural remodeling with delayed-enhancement magnetic resonance imaging in patients with atrial fibrillation. Circulation 2009;119:1758–1767.
26. Lustig M, Donoho D, Pauly JM. Sparse MRI: the application of compressed sensing for rapid MR imaging. Magn Reson Med 2007;58:1182–1195.

27. Block KT, Uecker M, Frahm J. Undersampled radial MRI with multiple coils. Iterative image reconstruction using a total variation constraint. Magn Reson Med 2007;57:1086–1098.
28. Akcakaya M, Rayatzadeh H, Basha TA, Hong SN, Chan RH, Kissinger KV, Hauser TH, Josephson ME, Manning WJ, Nezafat R. Accelerated late gadolinium enhancement cardiac MR imaging with isotropic spatial resolution using compressed sensing: initial experience. Radiology 2012;264:691–699.
29. Danias PG, Stuber M, Botnar RM, Kissinger KV, Chuang ML, Manning WJ. Navigator assessment of breath-hold duration: impact of supplemental oxygen and hyperventilation. AJR Am J Roentgenol 1998;171:395–397.
30. McCarthy RM, Shea SM, Deshpande VS, Green JD, Pereles FS, Carr JC, Finn JP, Li D. Coronary MR angiography: true FISP imaging improved by prolonging breath holds with preoxygenation in healthy volunteers. Radiology 2003;227:283–288.
31. Klocke FJ, Rahn H. Breath holding after breathing of oxygen. J Appl Physiol 1959;14:689–693.
32. Marks B, Mitchell DG, Simelaro JP. Breath-holding in healthy and pulmonary-compromised populations: effects of hyperventilation and oxygen inspiration. J Magn Reson Imaging 1997;7:595–597.
33. Holland AE, Goldfarb JW, Edelman RR. Diaphragmatic and cardiac motion during suspended breathing: preliminary experience and implications for breath-hold MR imaging. Radiology 1998;209: 483–489.
34. Look DC, Locker DR. Time saving in measurement of NMR and EPR relaxation times. Rev Sci Instrum 1970;41:250–251.
35. Wang Y, Riederer SJ, Ehman RL. Respiratory motion of the heart: kinematics and the implications for the spatial resolution in coronary imaging. Magn Reson Med 1995;33:713–719.
36. Akcakaya M, Basha TA, Goddu B, Goepfert LA, Kissinger KV, Tarokh V, Manning WJ, Nezafat R. Low-dimensional-structure self-learning and thresholding: regularization beyond compressed sensing for MRI reconstruction. Magn Reson Med 2011;66:756–767.
37. Gay SB, Sistrom CL, Holder CA, Suratt PM. Breath-holding capability of adults. Implications for spiral computed tomography, fast-acquisition magnetic resonance imaging, and angiography. Invest Radiol 1994;29:848–851.
38. Ordovas KG, Higgins CB. Delayed contrast enhancement on MR images of myocardium: past, present, future. Radiology 2011;261: 358–374.
39. Buchanan GF, Richerson GB. Role of chemoreceptors in mediating dyspnea. Respir Physiol Neurobiol 2009;167:9–19.
40. Manning HL, Schwartzstein RM. Pathophysiology of dyspnea. N Engl J Med 1995;333:1547–1553.
41. Parkes MJ. Breath-holding and its breakpoint. Exp Physiol 2006;91:1–15.